Hindawi Publishing Corporation
Journal of Chemistry
Volume 2016, Article ID 7296858, 13 pages
http://dx.doi.org/10.1155/2016/7296858

Research Article

Removal of Fluoride from Aqueous Solutions Using Chitosan Cryogels

Anete Jessica Arcos-Arévalo,[1] Rosa Elvira Zavala-Arce,[1] Pedro Ávila-Pérez,[2] Beatriz García-Gaitán,[1] José Luis García-Rivas,[1] and María de la Luz Jiménez-Núñez[1]

[1]*Tecnológico Nacional de México/Instituto Tecnológico de Toluca, Avenida Tecnológico S/N, Colonia Agrícola Bella Vista, 52149 Metepec, MEX, Mexico*
[2]*Dirección de Investigación Tecnológica, Instituto Nacional de Investigaciones Nucleares (ININ), Carretera México-Toluca S/N, La Marquesa, 52750 Ocoyoacac, MEX, Mexico*

Correspondence should be addressed to Rosa Elvira Zavala-Arce; rzavalaa@toluca.tecnm.mx

Received 22 July 2016; Accepted 21 November 2016

Academic Editor: Julie J. M. Mesa

In this study, crosslinked chitosan cryogels (QE) and chitosan's cryogels modified with iron (QEFe) were synthesized. They were characterized by BET, PZC, FTIR, and XPS spectroscopies. Results show a specific surface area of 36.67 and 29.17 $m^2 g^{-1}$ and 7.0 and 6.1 of PZC for the cryogels QE and QEFe, respectively. FTIR results show the characteristic bands of amino and hydroxyl groups, while in the XPS analysis, interactions between iron and oxygen with fluorine were observed. The removal of fluoride at temperatures of 303, 313, and 323 K in cryogels was tested. The Ho model is the best fit for the experimental data, suggesting that there is a chemisorption process involved in the removal of fluoride. The Langmuir-Freundlich model is the best to represent the behavior of the cryogels, and it is used to sorbents with heterogeneous surfaces. A maximum fluoride adsorption capacity of 280 and 295 mg F^-/g for QE and QEFe, respectively, at 303 K was obtained, showing that the removal of fluoride is favored by the iron incorporated in the polymer matrix of the cryogels. The thermodynamic parameters were obtained for both cryogels, where the values of ΔH° and ΔG° indicate that both systems are endothermic and nonspontaneous.

1. Introduction

The most abundant halogen in the Earth's crust is fluorine, with a concentration close to 0.3 g/kg. Diverse minerals contain fluorine in the form of fluorides [1, 2]. Aqueous solubilization of molecules containing fluorine occurs through geochemical processes. The regional geomorphic composition determines the amount of fluorine that reaches the aquifers [1–5]. The presence of fluorine affects the water quality for human consumption. Fluorine is highly reactive and therefore forms compounds with practically all the elements. Biologically active compounds are likely to incorporate fluorine when ingested in water for long periods. Epidemiological studies prove detrimental to the bone tissue (bones and teeth) and the spinal cord and brain. The degeneration of neurons and alteration of the metabolism of free radicals in the liver, kidney, and heart and lesions on the thyroid and the endocrine glands interfere with DNA synthesis, and metabolic disorders in soft tissues and some cancers are also associated with the exposure to fluorine [1–14]. The World Health Organization (WHO) classifies fluorine as a public health risk and recommends a maximum concentration of 1.5 mg/L of fluorine in drinking water. Globally, inhabitants in some regions of China, India, Mexico, and the United States are affected by higher concentrations [1, 2, 6–8, 12, 13].

In an effort to remove fluorine in water, diverse techniques have been studied, with absorption being the more versatile due to its high efficiency, sludge minimization, and regeneration of the sorbent material [6, 10, 15–18]. In recent years, biopolymers such as chitosan have proved to be effective for fluorine removal. Chitosan is a nontoxic, biodegradable, and biocompatible material [7]. Among the fluoride removal studies that have been used, sorbents from

chitosan inferred that these biosorbents offer satisfactory results in terms of fluoride elimination. In addition, chitosan is obtained from natural sources that are an ecologically low cost material [19–23]. The biopolymer structure consists of amino and hydroxyl groups which are mainly responsible for the adsorption of various ions [11, 16, 24, 25]. Also, limited swelling of chitosan in water causes low availability of its functional groups during sorption. Chemical and physical modifications improve the readiness of contact sites on chitosan [26, 27]. The cryogel synthesis route allows the structural transformations supplying adequate stability and strength to the material. Cryogels are porous materials that can provide a better contact surface between the functional groups of chitosan and different ions in aqueous solutions [28–33], so these materials are a suitable alternative for removal of fluoride ions in aqueous solutions.

The aim of this work was to synthesize chitosan's cryogels crosslinked with ethylene glycol diglycidyl ether (EGDE) and its modification with iron, in order to use them in the removal of fluoride from aqueous solutions prepared in the laboratory. A comparative assessment of the modified cryogels (QEFe) and unmodified cryogels (QE) was performed to determine the sorption capacity of each material and observe whether introducing Fe^{3+} into the chitosan polymeric matrix had a significant impact on the adsorption phenomenon.

2. Experimental

Industrial chitosan (América Alimentos) with 67% of deacetylation, ethylene glycol diglycidyl ether (TCI), $FeCl_3{\cdot}6H_2O$ (Sigma-Aldrich), ethanol (Meyer), and glacial acetic acid (Fermont) were used without further purification on cryogel synthesis. Sodium fluoride (Meyer) was used for preparing solutions in the sorption experiments.

2.1. Synthesis of Crosslinked Chitosan Cryogels (QE). Two solutions dissolving chitosan (Q) in 100 mL of acetic acid (3%) were prepared. Afterwards, the ethylene glycol diglycidyl ether as a cross-linking agent (E) was added at 1% relative to the chitosan weight under inert atmosphere and constant stirring during a 6-hour period. Each one of the solutions was dripped into liquid nitrogen and the obtained spheres were freeze-dried by using a lyophilizer CHRIST BETA 2-8 LD to 0018 mbar and 190 K for 17 hours. Finally, QE cryogels were washed with 1.5% acetic acid and then with deionized water until the rinse water's pH was equal to the pH of the deionized water.

2.2. Synthesis of Chitosan's Cryogels Modified with Iron (QEFe). The total QE cryogels obtained by one of the solutions in the synthesis of crosslinked chitosan cryogels were treated with 300 mL of solution 0.1 M $FeCl_3$ during a 24-hour period, with constant stirring at 303 K. Subsequently, the modified beads were washed with ethanol for removing the unreacted $FeCl_3$, followed by washing with deionized water until the rinse water pH was equal to the pH of the deionized water [26, 34].

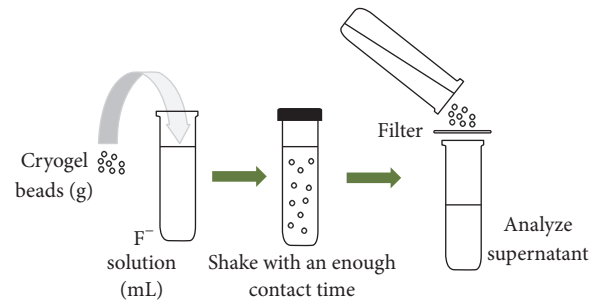

Figure 1: Experimental procedure for adsorption experiments.

2.3. Sorption Experiments. Sorption kinetics were performed in batch systems, putting a sample of each dried cryogel (0.002 g) in contact with 8 mL of a solution with an initial concentration of 10 mg/L of fluoride and pH = 6. Samples were placed at constant agitation of 200 rpm during a 24-hour period. Experiments were carried out at three constant temperatures (303 K, 313 K, and 323 K) to analyze the effect of this variable on sorption capacity (Figure 1). Furthermore, the effect of different fluoride initial concentrations was studied using 2 mg/L to 1000 mg/L at 303 K, 313 K, and 323 K. The adsorbent mass (0.002 g) was kept constant as well as pH value with a study solution volume of 8 mL. Fluoride ions in the solutions were quantified by using a Cole-Parmer 27504-14 selective ion electrode and a Thermo Scientific Orion 4-Star potentiometer. All experiments were triplicated under identical conditions. Finally, experimental data was fitted to mathematical models with nonlinear regression, using the Origin 8.1 program.

2.4. Characterization of Cryogels. The BET method was used with a Belsorp-max equipment to determine the specific surface area of cryogels. Before the analyses, the samples were subject to a degassing process in a Belprep II equipment, at a temperature of 373 K for 2 hours in order to remove impurities and water molecules contained in the material structure. Subsequently, each sample was weighed and placed in the Belsorp-max to carry out the determination of specific area through process of adsorption and desorption of N_2 gas at 77 K and 76.5 kPa.

The PZC was determined by means of contacting 0.5 g of the solid sample of cryogels (QE and QEFe) with 20 mL of NaCl solution 0.1 M at different pHs. The initial pH values of the solutions were adjusted using HCl or NaOH 0.1 M. The suspensions were then shaken for 24 hours (200 rpm and at 303 K), after which the pH value of the supernatant for each sample was measured. The difference between the final and initial pH ($\Delta pH = pH_f - pH_i$) was plotted versus pH_i and the point of intersection of the resulting curve at which $\Delta pH = 0$ was the pH_{PZC} value.

A FTIR spectrometer Variant 600 with an ATR-coupled device was used in order to identify the presence of the functional groups in chitosan-modified molecule by crosslinking in the adsorbent materials before (QEFe and QE) and after ($QEFe/F^-$ and QE/F^-) sorption. Sixteen scans were performed in a range of 4000–500 cm^{-1} with a resolution of 4 cm^{-1}.

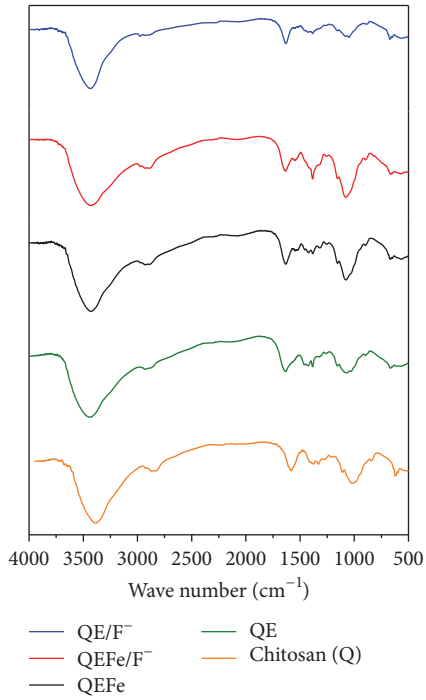

Figure 2: FTIR spectra.

An XPS spectrometer Thermo K-Alpha Scientific was also used to further verify the existence of study species in the materials, and the spectra were subjected to a mathematical deconvolution and an analysis of presented chemical interactions by using the Origin 8.1 program and the http://lasurface.com database.

3. Results and Discussion

3.1. Characterization of Cryogels. The specific surface area of cryogels was determined by the BET method. The specific surface areas for QE and QEFe cryogels were 36.67 m^2g^{-1} and 29.17 m^2g^{-1}, respectively.

In the infrared spectrum (Figure 2), vibrations of the different functional groups at the chitosan can be observed. In 3433 cm^{-1} band one is observed due to vibration of NH_2 and in 2922 cm^{-1} a band is observed due to vibration of OH; at 1633 cm^{-1} and 1420 cm^{-1} the vibration signals are present of NH_2 and OH, respectively. The spectra of the QE and QEFe cryogels have higher Q spectrum bands, virtually unchanged, showing that these functional groups are present in the cryogels. However, a decrease in signal intensity can be observed in the QEFe cryogel corresponding to the amino groups, which may indicate that the added iron is attached mainly by these functional groups. The cryogels spectra after fluoride sorption (QE/F^- and QEFe/F^-) show a decrease in the intensity of signal corresponding to the amino and hydroxyl groups. The hydroxyl group was the most decreased. This suggests that these groups are related to the removal of fluoride ions [35, 36].

The cryogels were analyzed by XPS before (QEFe and QE) and after (QEFe/F^- and QE/F^-) the sorption of fluoride ions. C, O, N, Fe, and F were identified in both samples. Figures 3 and 4 show the XPS results before and after the sorption of each material, where the predominant peaks C1s and O1s and a lower intensity peak N1s can be observed. These can be attributed to the amino groups of chitosan. In the case of QEFe cryogel, the presence of Fe2p can also be observed. After the sorption, the peak of F1s appears to show an average binding energy of about 690 eV, meaning that fluoride was adsorbed on the surface of both cryogels [37, 38].

Figures 5, 6, and 7 show the deconvolution of the O1s and Fe2p spectrums after the sorption with QE and QEFe cryogels. Here, it can be observed that fluoride ions are interacting with the atoms of iron and oxygen in the materials; that is, fluorine is showing bonds with the hydroxyl group of the cryogels, which can be hydrogen bonds. In the case of the QEFe cryogel, it is also forming links with the iron present in the modified cryogel. These interactions may be because the QEFe cryogel presents a higher sorption capacity than the cryogel QE [39, 40].

Figure 8 shows the PZC results. When the pH of the solution is lower than the PZC, the total charge of the solid surface is positive, while if the pH of the solution is greater than the PZC, the surface is negatively charged [41, 42]. The cryogel QEFe showed a less slightly acidic PZC compared to the cryogel QE (6.1 and 7.0, resp.), which can indicate that, in the first one, the content of total acid groups is greater than the content of basic groups.

The pH of the washing solution of cryogels (QE and QEFe) is pH 5 and according to the PZC, both cryogels have a positive charge on their surface; because of this, the removal mechanism of fluorine in the QE cryogel is mainly a physical adsorption by the formation of hydrogen bonds between fluoride and the hydroxyl group and in the QEFe cryogel is a physical and chemical adsorption mainly due to interactions between iron and fluoride (Figure 9) [21, 34, 43, 44].

3.2. Sorption Kinetics. The quality of the sorbent material is evaluated according to the capacity to retain certain species on its surface. For the purpose, it is customary to determine the amount of species removed per unit of solid phase (q) and the following equation is used:

$$q = \frac{\left(C_i - C_f\right) * V}{m}, \tag{1}$$

where C_i and C_f are the initial and final concentrations (mgL^{-1}), respectively, V is the total volume (L), and m is the amount of solid added (g).

In general, the removal of ions from aqueous solutions depends on the chemical mechanisms that involve the interaction of ions with the active groups present in the sorbent. Therefore, the kinetics show the steps through which the sorption takes place. In this paper, Lagergren, Elovich, and Ho models have been considered.

The mathematical expression for the kinetics of pseudo-first-order or Lagergren model is based on the assumption

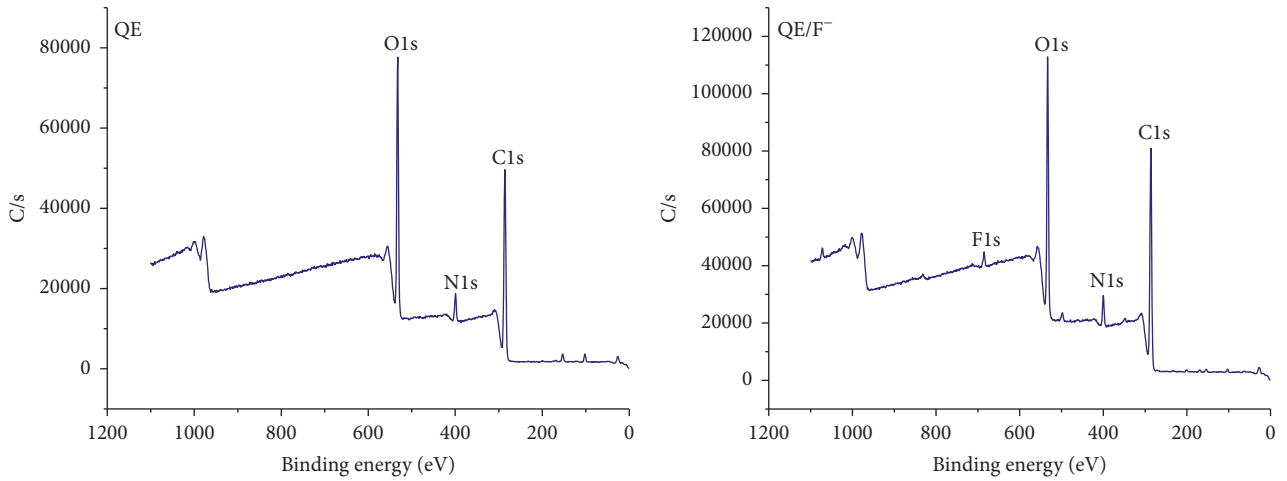

Figure 3: XPS spectrums of QE and QE/F⁻.

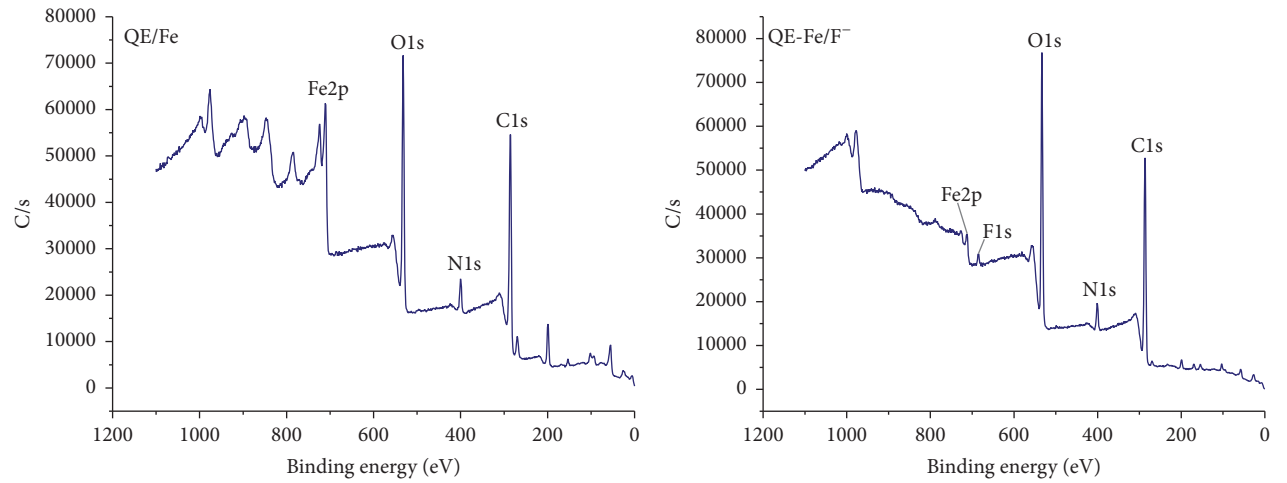

Figure 4: XPS spectrums of QEFe and QEFe/F⁻.

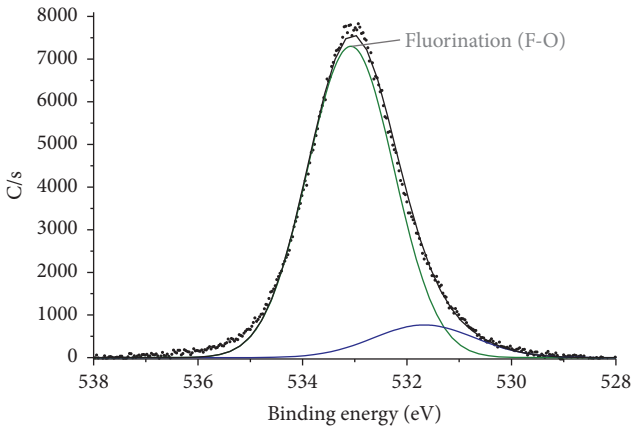

Figure 5: XPS spectrum to O1s of QE/F⁻.

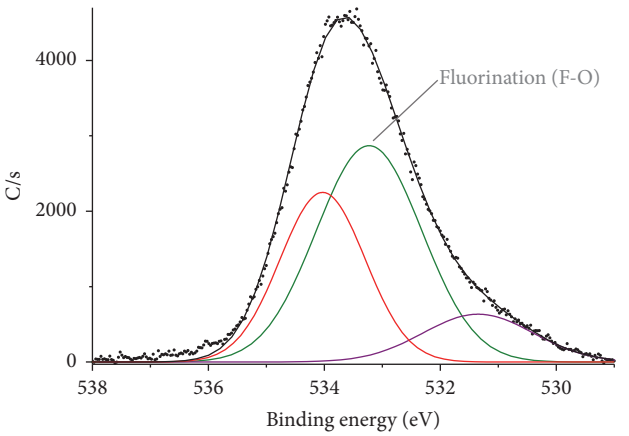

Figure 6: XPS spectrum to O1s of QEFe/F⁻.

Table 1: Summary of kinetics models.

T (K)	Cryogel	q_{exp} (mgg^{-1})	Lagergren			Ho			Elovich		
			R^2	K_1 (min^{-1})	q_e (mgg^{-1})	R^2	K_2 (gmg^{-1}min^{-1})	q_e (mgg^{-1})	R^2	α (mgg^{-1}h^{-1})	β (gmg^{-1})
303	QE	13.10	0.98	0.44	13.89	0.97	0.15	13.94	0.96	8.54×10^{44}	8.04
	QEFe	23.20	0.98	0.20	22.09	0.98	0.02	22.71	0.96	5.55×10^{5}	0.84
313	QE	15.80	0.88	0.26	14.20	0.94	2.30×10^{-2}	14.83	0.99	5.29×10^{3}	0.97
	QEFe	24.20	0.98	0.32	23.02	0.99	3.40×10^{-2}	23.37	0.98	4.65×10^{11}	1.42
323	QE	11.20	0.80	0.03	10.34	0.87	5.00×10^{-3}	10.81	0.94	6.977	0.76
	QEFe	14.50	0.99	0.20	14.62	0.97	0.03	14.91	0.91	1.32×10^{9}	1.88

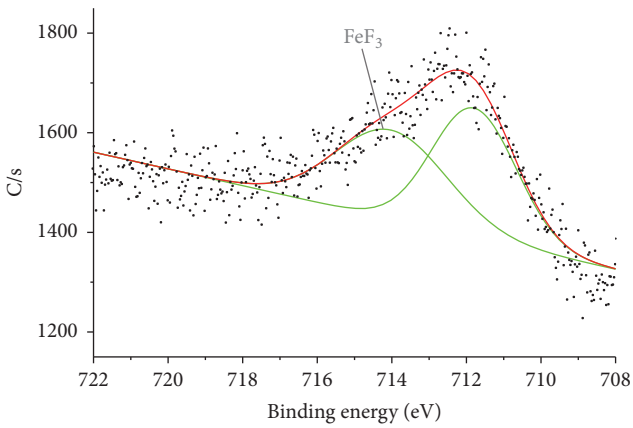

Figure 7: XPS spectrum to Fe2p of QEFe/F$^-$.

that each ion is assigned a sorption site of the sorbent material and it is represented [12, 45–47]:

$$q_t = q_e\left(1 - e^{-K_1 t}\right), \tag{2}$$

where K_1 is the sorption constant for pseudo-first-order model (min^{-1}), q_t is the mg of F$^-$ adsorbed/g of sorbent anytime, and q_e is the amount adsorbed on the equilibrium (mgg^{-1}).

The mathematical expression of Elovich model was developed for heterogeneous sorption processes of gas in solids. However, it has been successfully applied in processes of sorption for contaminants in solution, and the next equation describes this model [48–53]:

$$q_t = \frac{1}{\beta}\ln(\alpha\beta) + \frac{1}{\beta}\ln t, \tag{3}$$

where α is the initial sorption rate (mg g^{-1}h^{-1}), β is the desorption constant (gmg^{-1}), t is time (h), and q is the amount of solute sorbed (mgg^{-1}).

The Ho model was developed by Ho and McKay; it is assumed that the sorbate is adsorbed by two active sites in the sorbent. The next equation describes this model [45, 46, 52, 53]:

$$\frac{t}{q_t} = \frac{1}{(K_2)\,q_e^2} + \frac{t}{q_e}, \tag{4}$$

where K_2 is the pseudo-second-order constant (gmg^{-1} min^{-1}), q_t is the amount adsorbed anytime (or time, t) (mg g^{-1}), and q_e is the amount adsorbed on the equilibrium (mg g^{-1}).

The fluoride sorption occurs in the first 5 minutes of the test for both cryogels (Figure 10) and then begins to stabilize until equilibrium is reached. It was determined that the equilibrium time was reached approximately in 480 minutes for both cryogels. After reaching equilibrium, there were no significant changes in the quantity of fluorine captured by the materials. Furthermore, the QEFe cryogel exhibited a greater sorption capacity at the three temperatures studied than the QE cryogel.

After the sorption kinetics, an adjustment of the experimental data for the Lagergren, Elovich, and Ho models by means of nonlinear regression using the Origin 8.1 program was performed. Table 1 provides a summary of the obtained parameters.

The QE cryogel shows a higher R^2 coefficient in the Lagergren model at 303 K, whereas at 313 K and 323 K the coefficient is higher in the Elovich model. The QEFe cryogel shows a higher correlation coefficient for Ho model at 303 K and 313 K and for the Lagergren model at 323 K. According to Figure 11, the Ho model is what best fits the experimental data, suggesting that there is a chemisorption process involved in the removal of fluoride. As a result the model that best describes the behavior of the systems is the Ho model.

In other articles materials of chitosan have been used in order to remove fluoride and under similar conditions used in this study, such is the case of the chitosan beads modified by carboxylation followed by chelation with Fe^{3+} (4.23 mg F$^-$/g), the chitosan modified with a mixed of rare earths (3.72 mg F$^-$/g), a bioadsorbent of titanium(IV) hydrate based on chitosan template (11.44 mg F$^-$/g), and an Al-doping chitosan-Fe(III) hydrogel (3.9 mg F$^-$/g). The sorption capacity in equilibrium time is similar to or lower than sorption capacity obtained in this work: 13.10 mg F$^-$/g and 23.20 mg F$^-$/g at 303 K for the QE and QEFe cryogels, respectively [13, 34, 54, 55].

3.3. Sorption Isotherms. Over time, several mathematical models have been developed for the treatment of experimental data using the models of Langmuir, Freundlich, and Langmuir-Freundlich.

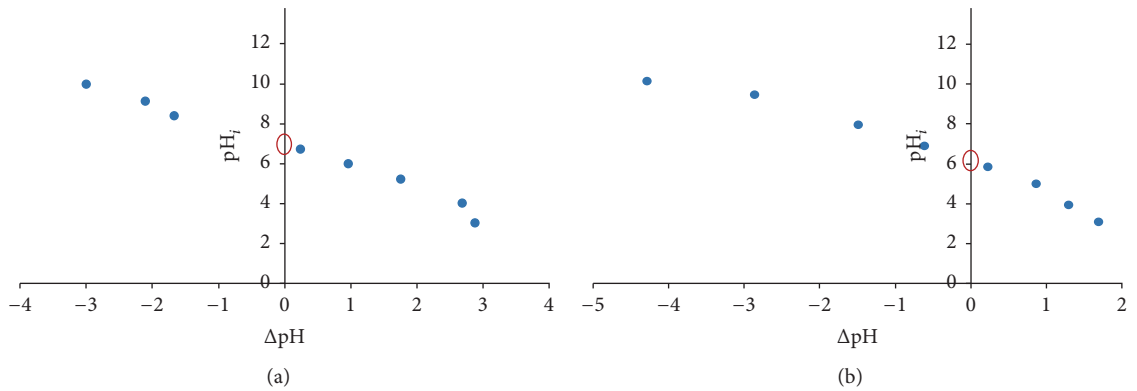

Figure 8: PZC of cryogels, 0.5 g cryogel mass, 20 mL NaCl solution at various pHs, 200 rpm, 303 K, a 24-hour period, closed atmosphere: (a) QE and (b) QEFe.

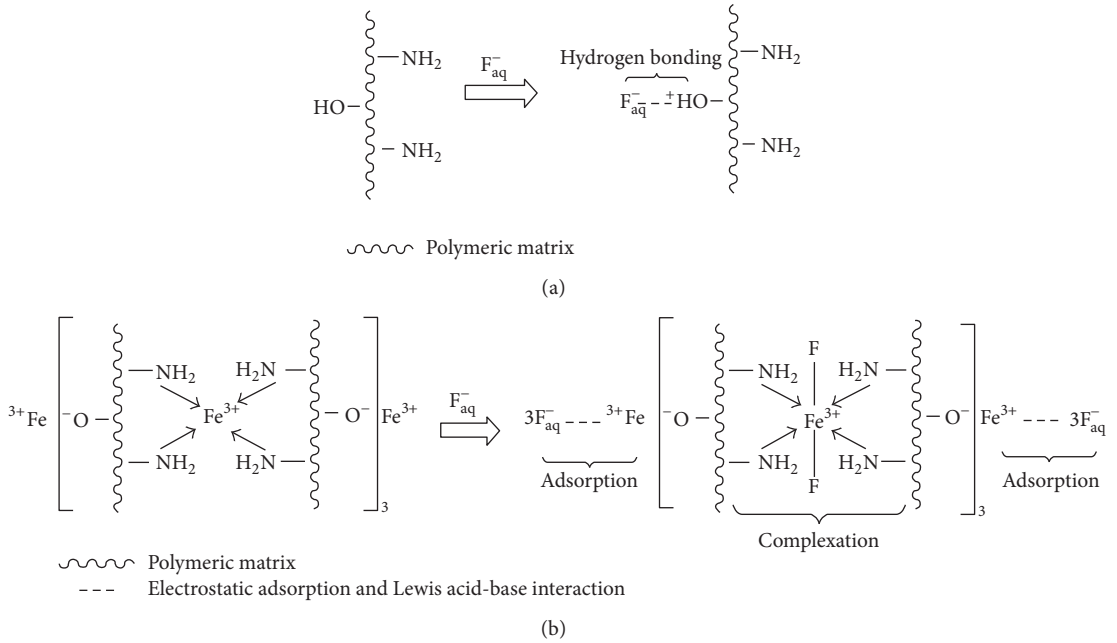

Figure 9: Fluoride removal mechanism (adapted from Viswanathan and Meenakshi [34]): (a) interaction with OH, (b) interaction with Fe.

The Freundlich model is an empirical model that can be applied to a nonideal adsorption in heterogeneous surfaces, as well as multilayer adsorption. The Freundlich model is expressed by the following equation [12, 13, 46–48]:

$$q_e = K_F C_e^{1/n}, \tag{5}$$

where q_e is the adsorption capacity at equilibrium (mgg^{-1}), K_F is the constant for Freundlich's isotherm (mgg^{-1}), C_e is the ion concentration in the solution at equilibrium (mgL^{-1}), $1/n$ is the quotient related to adsorption intensity, and n is the dimensionless exponent of the Freundlich isotherm.

The Langmuir model is probably the best-known and the most widely applied adsorption isotherm. This isotherm assumes that a solid has a limited adsorption capacity; the molecules are adsorbed on well-defined and energetically equivalent sites and are far enough away from each other to not allow interaction between the adsorbed molecules in adjacent sites. Each site can retain only one molecule of adsorbate and the sorption leads to the deposition of a layer of solute molecules on the surface of sorbent. The model can be represented by the following equation [46, 48–50, 56]:

$$q_e = \frac{q_m b C_e}{1 + b C_e}, \tag{6}$$

where q_e is the adsorption capacity at equilibrium (mgg^{-1}), q_m is the monolayer adsorption capacity (mgg^{-1}), b is the constant for Langmuir's isotherm (Lmg^{-1}), and C_e is the ion concentration in the solution at equilibrium (mgL^{-1}).

Langmuir also considered the case of a molecule occupying two sites and it produces the Sips or Langmuir-Freundlich isotherm. The Langmuir-Freundlich name is derived from

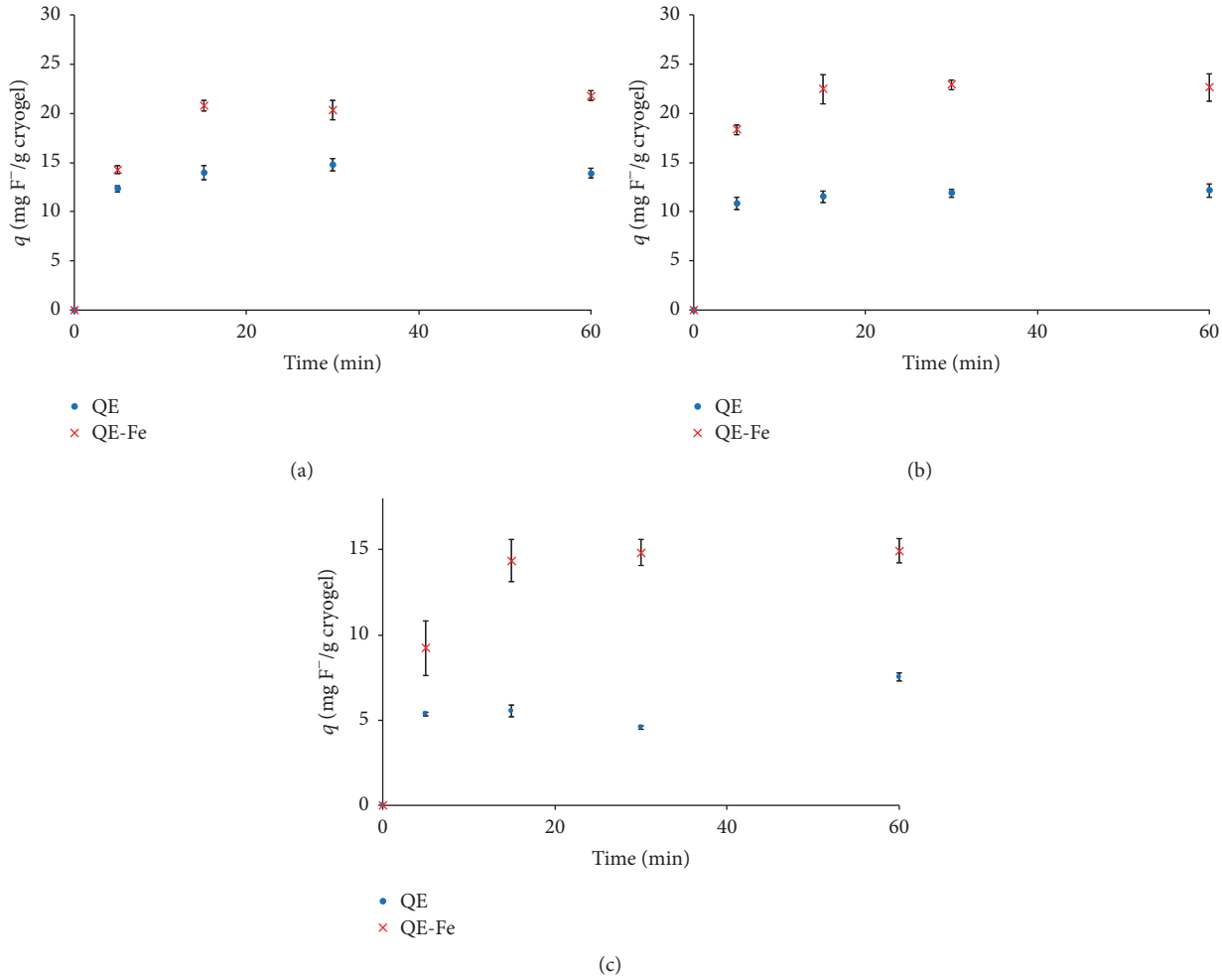

Figure 10: Sorption kinetics, 8 mL of 10 mgL^{-1}, 200 rpm, 0.002 g of cryogel mass, pH 6, closed atmosphere: (a) 303 K, (b) 313 K, and (c) 323 K.

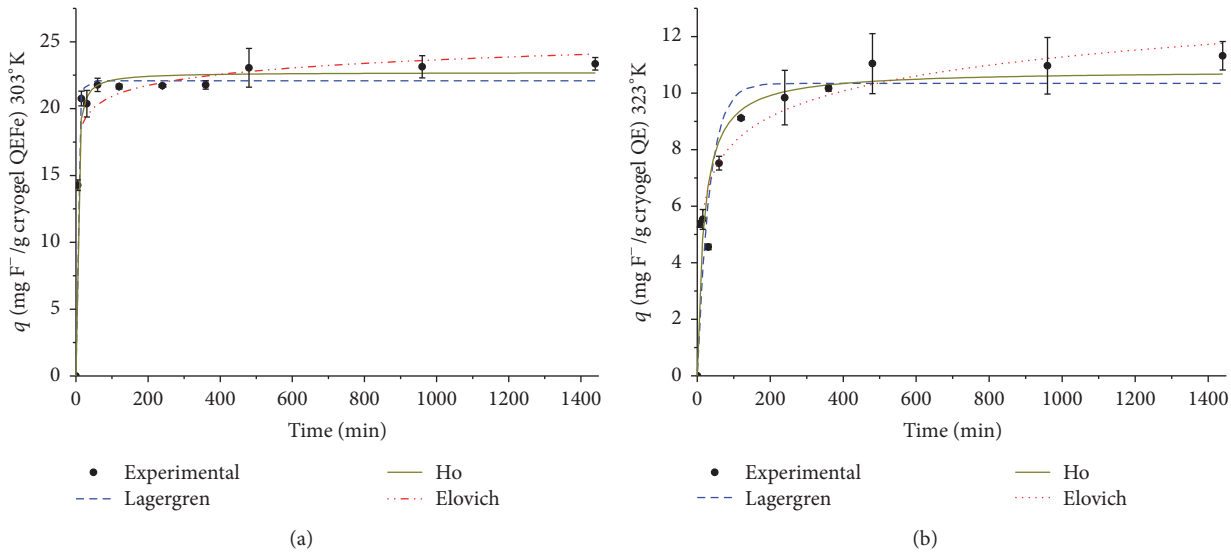

Figure 11: Adjustment to kinetics models, 8 mL of 10 mgL^{-1}, 200 rpm, 0.002 g cryogel mass, pH 6, closed atmosphere: (a) cryogel QEFe 303 K; (b) cryogel QE 323 K.

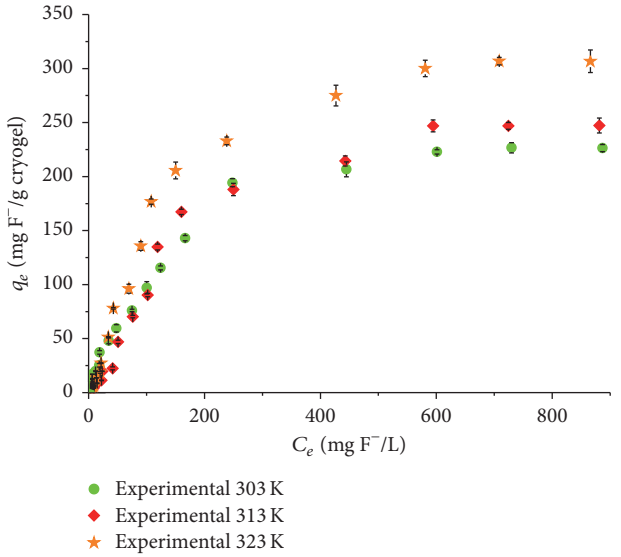

Figure 12: Sorption isotherms, cryogel QE, 8 mL, 24 hours of contact, 200 rpm, 0.002 g cryogel mass, pH 6, closed atmosphere.

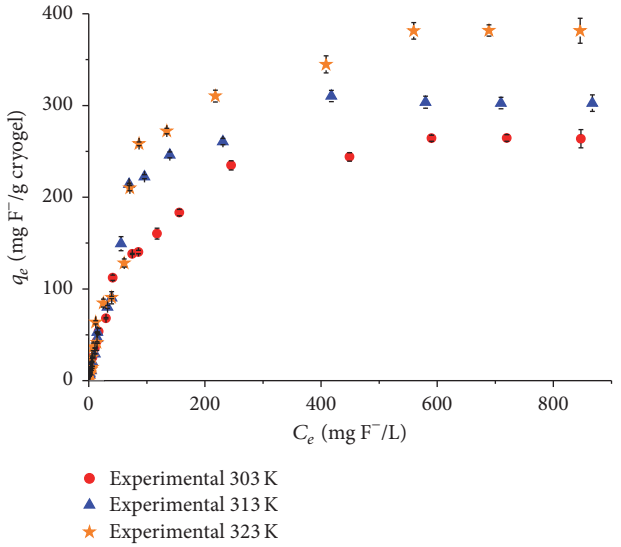

Figure 13: Sorption isotherms, cryogel QEFe, 8 mL, 24 hours of contact, 200 rpm, 0.002 g cryogel mass, pH 6, closed atmosphere.

the limiting behavior of the equation. At low sorbate concentrations it effectively reduces to a Freundlich isotherm. At high sorbate concentrations, it predicts the monolayer adsorption characteristic of the Langmuir isotherm [46, 57–60]. This isotherm can be determined by the following equation:

$$q_e = \frac{K_{LF}(C_e)^{n_{LF}}}{1 + (a_{LF}C_e)^{n_{LF}}}, \quad (7)$$

where q_e is the adsorption capacity at equilibrium (mgg^{-1}), a_{LF} is the constant of Langmuir-Freundlich's isotherm [$(Lmg^{-1})^{n_{LF}}$], C_e is the ion concentration in the solution at equilibrium (mgL^{-1}), K_{LF} is the constant of Langmuir-Freundlich's isotherm ($mg^{1-n_{LF}}L^{3n_{LF}}g^{-1}$), and n_{LF} is the dimensionless exponent of Langmuir-Freundlich's isotherm.

The isotherms do not show appreciable changes in adsorption capacity in a concentration of 500 mg/L of fluorine (Figures 12 and 13). In addition, it can be observed that the sorption capacities for both cryogels increase as the temperature increases; that is, the removal of fluoride ions was favored at higher temperatures, indicating an endothermic adsorption [15, 61].

Table 2 shows a summary of the values obtained after the adjustment of the experimental data to the models of Freundlich, Langmuir, and Langmuir-Freundlich, obtained by nonlinear regression and using the program Origin 8.1. Figures 14 and 15 show the data adjustment of these three models at the temperature of 323 K.

The identification of an adequate isotherm model can be carried out by means of the analysis of chi-square (χ^2), which uses the experimental data and the adjusted data by the isotherms models:

$$\chi^2 = \sum \left(\frac{(q_t - q_{tm})^2}{q_{tm}} \right), \quad (8)$$

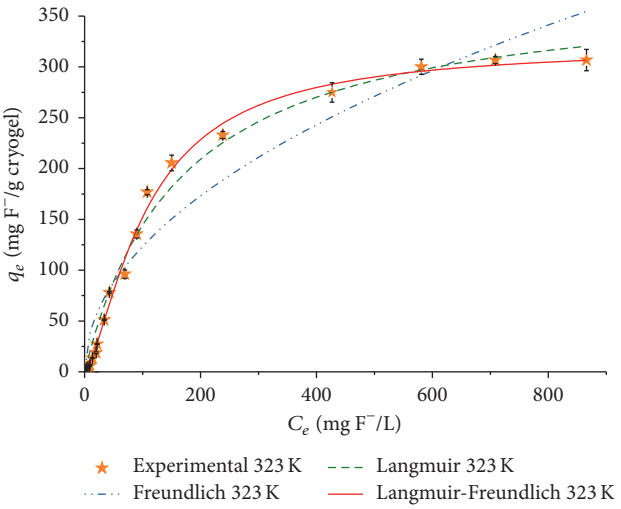

Figure 14: Sorption isotherms, cryogel QE fitted to Freundlich, Langmuir, and Langmuir-Freundlich models; 8 mL, 24 hours of contact, 200 rpm, 0.002 g cryogel mass, pH 6, T = 323 K, closed atmosphere.

where q_{tm} and q_t are the adsorption capacities obtained by the isotherm models and the experimental adsorption capacity (mgg^{-1}), respectively. When low values of χ^2 are observed, the experimental data has a good fit to the model used [15, 17, 34, 40, 44, 50, 53, 62].

A maximum fluoride adsorption capacity of 280 mg F$^-$/g for QE and 295 mg F$^-$/g for QEFe at 303 K was obtained, showing that the removal of fluoride is favored by the iron incorporated in the polymer matrix of the cryogels. The coefficients of determination are very similar in the Langmuir and Langmuir-Freundlich models (Table 2). The Chi-square test shows that the Langmuir and Langmuir-Freundlich models can adequately represent the experimental data because the

Table 2: Summary of isotherms.

T (K)	Cryogel	Freundlich					Langmuir				Langmuir-Freundlich				
		K_F [(mgg^{-1})(Lmg^{-1})$^{1/n}$]	n	$1/n$	R^2	χ^2	q_m (mgg^{-1})	b (Lmg^{-1})	R^2	χ^2	K_{LF} (mg^{1-n} L^{3n}g^{-1})	a	n	R^2	χ^2
303	QE	11.19	2.16	0.46	0.95	90.74	280.87	6×10^{-3}	0.99	17.23	1.13	4×10^{-3}	1.10	0.99	27.28
	QEFe	22.48	2.60	0.38	0.95	125.00	295.38	11×10^{-3}	0.99	10.33	4.13	14×10^{-3}	0.95	0.99	8.59
313	QE	7.56	1.86	0.54	0.93	194.89	330.35	4×10^{-3}	0.97	71.62	0.05	2×10^{-4}	1.76	0.99	41.57
	QEFe	23.86	2.66	0.37	0.94	133.97	291.19	13×10^{-3}	0.99	20.04	4.99	16×10^{-3}	0.92	0.99	17.41
323	QE	12.94	2.04	0.49	0.93	237.47	381.13	6×10^{-3}	0.99	66.71	0.35	1×10^{-3}	1.45	0.99	12.94
	QEFe	28.33	2.46	0.41	0.92	270.88	436.64	11×10^{-3}	0.98	54.53	2.11	5×10^{-3}	1.21	0.98	73.48

Table 3: Thermodynamic parameters.

Cryogel	ΔS° (J/Kmol)	ΔH° (J/mol)	$\Delta G^\circ_{303\,K}$ (J/mol)	$\Delta G^\circ_{313\,K}$ (J/mol)	$\Delta G^\circ_{323\,K}$ (J/mol)
QE	36.03	13472	2501	2287	1774
QEFe	49.41	17052	2024	1685	1029

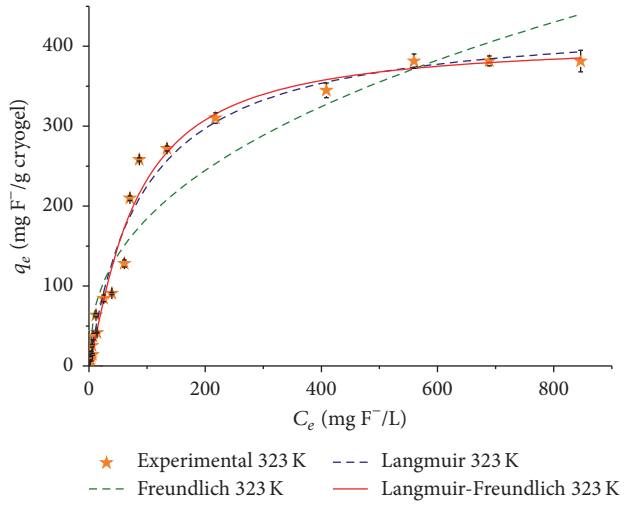

Figure 15: Sorption isotherms, cryogel QEFe fitted to Freundlich, Langmuir, and Langmuir-Freundlich models; 8 mL, 24 hours of contact, 200 rpm, 0.002 g cryogel mass, pH 6, T = 323 K, closed atmosphere.

lowest values of Chi-square are obtained by both models. However, the model that best represents the data obtained in terms of best fit to the experimental data is the Langmuir-Freundlich model, as shown in Figures 14 and 15. This model is applicable to adsorbents with heterogeneous surfaces. At low concentrations of sorbate, data is best adjusted by Freundlich's isotherm, while, at high concentrations of sorbate, data shows a monolayer adsorption and it is best adjusted by the Langmuir isotherm [47, 63]; this is consistent with the proposed removal mechanism in Section 3.1.

3.4. Thermodynamic Parameters. The thermodynamic parameters are used to estimate the feasibility of the adsorption process as well as the effect of temperature. The change in the standard Gibbs free energy (ΔG°) determines if a process is spontaneous or not.

The Van't Hoff equation is used to obtain graphically the values ΔH° and ΔS°. This equation arises from the equation of Gibbs free energy as follows:

$$\Delta G^\circ = -RT \ln K_C,$$
$$\ln K_C = \frac{-\Delta H^\circ}{RT} + \frac{\Delta S^\circ}{R}. \quad (9)$$

A plotting of $\ln K_C$ in the y-axis and T^{-1} on the x-axis should be lineal and the intercept would be equal to $\Delta S^\circ/R$, while the slope would be numerically equal to $-\Delta H^\circ/R$, where R (8.314 Jmol^{-1}K^{-1}) is the universal gas constant. Meanwhile K_C is determined as follows:

$$K_C = \frac{C_{Ae}}{C_{Se}}, \quad (10)$$

where C_{Ae} is equilibrium adsorbate concentration on the surface of the adsorbent and C_{Se} is the equilibrium concentration in the solution.

The standard enthalpy change (ΔH°) provides information about the exothermic or endothermic reaction, and finally the standard entropy change (ΔS°) predicts the magnitude of the changes on the adsorbent surface [15, 47, 49, 57, 61, 63–65].

Table 3 shows the results of the thermodynamic parameters. ΔS° suggests an increase in the disorder of the system and a more widespread disorder can be expected during sorption. The values of ΔH° indicate that these systems are endothermic, and because ΔH° is below 40 kJ/mol this suggests a coexistence of physical and chemical adsorption. Moreover, ΔG° suggest that the system is not spontaneous, so it is necessary to provide energy to the system [7, 13, 15, 16, 46, 52, 66, 67].

4. Conclusions

The X-ray photoelectron spectroscopy shows that fluoride groups interact with oxygen groups in the QE cryogel. Therefore, the fluoride presents links with the hydroxyl groups of the cryogels, which can be hydrogen bonds. Meanwhile, the QEFe cryogel shows interactions between iron and oxygen in the material, so the fluoride ions also form links with the iron by means of hydrogen bonds. The QEFe cryogel shows a higher sorption capacity for fluorides than the QE cryogel.

The QE and QEFe cryogels have a similar adsorption capacity. However, the QEFe cryogel shows the highest adsorption capacity. The sorption kinetics show that the Ho model fits the data better than the Elovich and Lagergren models, which suggests that the removal mechanism also involves chemical adsorption. The sorption isotherms show that the Langmuir-Freundlich model best represents the experimental data and the behavior of cryogels. The point of zero charge shows that on the surface of the cryogels it has predominantly positive charges; because of this, the removal mechanism of fluorine in the QE cryogel is mainly the physical adsorption type and in the QEFe cryogel is a physical and chemical adsorption. Finally, the thermodynamic parameters show that the systems are endothermic and nonspontaneous and there is a coexistence of physical and chemical adsorption.

Competing Interests

The authors declare that they have no competing interests.

Acknowledgments

The authors acknowledge sincerely Direction General of Technological Superior Education (DGEST) by the support (Code 5194.13-P), National Council for Science and Technology (CONACYT) for granting the fellowship of one of the authors, Miss Arcos-Arévalo, National Institute for Nuclear Research (ININ) for the facilities to perform this study, and also Mr. Rafael Basurto Sánchez of the physics department (ININ) and Mrs. Elvia Morales Moreno of the chemistry department (ININ) for their support in the XPS and FTIR analysis.

References

[1] Agencia para Sustancias Tóxicas y el Registro de Enfermedades (ATSDR), *Reseña Toxicológica del Cobre*, Departamento de Salud y Servicios Humanos de los EE.UU., Servicio de Salud Pública, Atlanta, Ga, USA, 2004.

[2] Organización Mundial de la Salud, *Guías para la Calidad del Agua Potable. Primer Apéndice a la Tercera Edición*, vol. 1, Organización Mundial de la Salud, Geneva, Switzerland, 2006.

[3] L. Galicia-Chacón, A. Molina-Frechero, A. Oropeza-Oropeza, E. Gaona, and L. Juárez-López, "Análisis de la concentración de fluoruro en agua potable de la delegación Tláhuac, Ciudad de México," *Revista Internacional de Contaminación Ambiental*, vol. 27, no. 4, 2011.

[4] R. Trejo-Vázquez, J. R. Treviño-Díaz, and E. García-Díaz, "Contaminación aguda por fluoruros en Aguascalientes," Conciencia Tecnológica 36, Instituto Tecnológico de Aguascalientes, Aguascalientes, México, 2008.

[5] S. Vega-Gleason, *Riesgo sanitario ambiental por la presencia de arsénico y fluoruros en los acuíferos de México*. Comisión Nacional del Agua, Gerencia de Saneamiento y Calidad del Agua, 2012.

[6] S. K. Swaina, T. Patnaik, P. C. Patnaik, U. Jha, and R. K. Dey, "Development of new alginate entrapped Fe(III)–Zr(IV) binary mixed oxide for removal of fluoride from water bodies," *Chemical Engineering Journal*, vol. 215-216, pp. 763–771, 2013.

[7] M. Karthikeyan, K. K. S. Kumar, and K. P. Elango, "Batch sorption studies on the removal of fluoride ions from water using eco-friendly conducting polymer/bio-polymer composites," *Desalination*, vol. 267, no. 1, pp. 49–56, 2011.

[8] N. Viswanathan and S. Meenakshi, "Selective fluoride adsorption by a hydrotalcite/chitosan composite," *Applied Clay Science*, vol. 48, no. 4, pp. 607–611, 2010.

[9] V. Tomar, S. Prasad, and D. Kumar, "Adsorptive removal of fluoride from water samples using Zr-Mn composite material," *Microchemical Journal*, vol. 111, pp. 116–124, 2013.

[10] V. Tomar, S. Prasad, and D. Kumar, "Adsorptive removal of fluoride from aqueous media using citrus limonum (lemon) leaf," *Microchemical Journal*, vol. 112, pp. 97–103, 2014.

[11] D. Thakre, S. Jagtap, A. Bansiwal, N. Labhsetwar, and S. Rayalu, "Synthesis of La-incorporated chitosan beads for fluoride removal from water," *Journal of Fluorine Chemistry*, vol. 131, no. 3, pp. 373–377, 2010.

[12] K. Biswas, K. Gupta, A. Goswami, and U. C. Ghosh, "Fluoride removal efficiency from aqueous solution by synthetic iron(III)-aluminum(III)-chromium(III) ternary mixed oxide," *Desalination*, vol. 255, no. 1–3, pp. 44–51, 2010.

[13] J. Liu, W.-Y. Li, Y. Liu, Q. Zeng, and S. Hong, "Titanium(IV) hydrate based on chitosan template for defluoridation from aqueous solution," *Applied Surface Science*, vol. 293, pp. 46–54, 2014.

[14] J. J. García-Sánchez, M. Solache-Ríos, V. Martínez-Miranda, and C. Solís Morelos, "Removal of fluoride ions from drinking water and fluoride solutions by aluminum modified iron oxides in a column system," *Journal of Colloid and Interface Science*, vol. 407, pp. 410–415, 2013.

[15] M. G. Sujana, A. Mishra, and B. C. Acharya, "Hydrous ferric oxide doped alginate beads for fluoride removal: adsorption kinetics and equilibrium studies," *Applied Surface Science*, vol. 270, pp. 767–776, 2013.

[16] S. Jagtap, D. Thakre, S. Wanjari, S. Kamble, N. Labhsetwar, and S. Rayalu, "New modified chitosan-based adsorbent for defluoridation of water," *Journal of Colloid and Interface Science*, vol. 332, no. 2, pp. 280–290, 2009.

[17] N. Viswanathan and S. Meenakshi, "Enriched fluoride sorption using alumina/chitosan composite," *Journal of Hazardous Materials*, vol. 178, no. 1-3, pp. 226–232, 2010.

[18] H. Paudyal, B. Pangeni, K. Inoue et al., "Adsorptive removal of trace concentration of fluoride ion from water by using dried orange juice residue," *Chemical Engineering Journal*, vol. 223, pp. 844–853, 2013.

[19] S. Annouar, M. Mountadar, A. Soufiane, A. Elmidaoui, and M. A. M. Sahli, "Defluoridation of underground water by adsorption on the chitosan and by electrodialysis," *Desalination*, vol. 165, p. 437, 2004.

[20] A. Bhatnagar, E. Kumar, and M. Sillanpää, "Fluoride removal from water by adsorption—a review," *Chemical Engineering Journal*, vol. 171, no. 3, pp. 811–840, 2011.

[21] P. Miretzky and A. Fernandez-Cirelli, "Fluoride removal from water by chitosan derivatives and composites: a review," *Journal of Fluorine Chemistry*, vol. 132, no. 4, pp. 231–240, 2011.

[22] N. Viswanathan, C. S. Sundaram, and S. Meenakshi, "Removal of fluoride from aqueous solution using protonated chitosan beads," *Journal of Hazardous Materials*, vol. 161, no. 1, pp. 423–430, 2009.

[23] R. Huang, B. Yang, Q. Liu, and K. Ding, "Removal of fluoride ions from aqueous solutions using protonated cross-linked chitosan particles," *Journal of Fluorine Chemistry*, vol. 141, pp. 29–34, 2012.

[24] S. Jagtap, M. K. Yenkie, S. Das, and S. Rayalu, "Synthesis and characterization of lanthanum impregnated chitosan flakes for fluoride removal in water," *Desalination*, vol. 273, no. 2-3, pp. 267–275, 2011.

[25] D. H. K. Reddy and S.-M. Lee, "Application of magnetic chitosan composites for the removal of toxic metal and dyes from aqueous solutions," *Advances in Colloid and Interface Science*, vol. 201-202, pp. 68–93, 2013.

[26] C. Jeon and W. H. Höll, "Chemical modification of chitosan and equilibrium study for mercury ion removal," *Water Research*, vol. 37, no. 19, pp. 4770–4780, 2003.

[27] C. Shen, H. Chen, S. Wu et al., "Highly efficient detoxification of Cr(VI) by chitosan-Fe(III) complex: process and mechanism studies," *Journal of Hazardous Materials*, vol. 244-245, pp. 689–697, 2013.

[28] X. Wang and B. G. Min, "Cadmium sorption properties of poly (vinyl alcohol)/hydroxyapatite cryogels: I. kinetic and isotherm studies," *Journal of Sol-Gel Science and Technology*, vol. 43, no. 1, pp. 99–104, 2007.

[29] X. Wang and B. G. Min, "Cadmium sorption properties of poly(vinyl alcohol)/hydroxyapatite cryogels: II. Effects of operating parameters," *Journal of Sol-Gel Science and Technology*, vol. 45, no. 1, pp. 17–22, 2008.

[30] I. E. Veleshko, V. V. Nikonorov, A. N. Veleshko et al., "Sorption of Eu(III) from solutions of covalently cross-linked chitosan cryogels," *Fibre Chemistry*, vol. 42, no. 6, pp. 364–369, 2011.

[31] V. V. Nikonorov, R. V. Ivanov, N. R. Kil'deeva, L. N. Bulatnikova, and V. I. Lozinskii, "Synthesis and characteristics of cryogels of chitosan crosslinked by glutaric aldehyde," *Polymer Science Series A*, vol. 52, no. 8, pp. 828–834, 2010.

[32] K. Tekin, L. Uzun, Ç. A. Şahin, S. Bektaş, and A. Denizli, "Preparation and characterization of composite cryogels containing imidazole group and use in heavy metal removal," *Reactive & Functional Polymers*, vol. 71, no. 10, pp. 985–993, 2011.

[33] R. Garcia-Gonzalez, R. R. E. Zavala-Arce, P. Avila-Perez et al., "Síntesis y caracterización de un material criogénico a partir de quitosano y celulosa," *Afinidad*, vol. 71, no. 567, 2014.

[34] N. Viswanathan and S. Meenakshi, "Selective sorption of fluoride using Fe(III) loaded carboxylated chitosan beads," *Journal of Fluorine Chemistry*, vol. 129, no. 6, pp. 503–509, 2008.

[35] C. J. Creswell, O. Runquist, and M. M. Campbell, Editorial Diana, México, 1972.

[36] G. Brust, *Espectroscopía Infrarroja*, Universidad del Sur de Mississippi, 1997.

[37] A. Bismarck, R. Tahhan, J. Springer et al., "Influence of fluorination on the properties of carbon fibres," *Journal of Fluorine Chemistry*, vol. 84, no. 2, pp. 127–134, 1997.

[38] C. D. Wagner, J. F. Moulder, L. E. David, and W. M. Riggs, *Handbook of X-Ray Photoelectron Spectroscopy*, Perkin-Elmer, Norwalk, Conn, USA, 1989.

[39] N. Viswanathan, C. Sairam Sundaram, and S. Meenakshi, "Development of multifunctional chitosan beads for fluoride removal," *Journal of Hazardous Materials*, vol. 167, no. 1-3, pp. 325–331, 2009.

[40] N. Viswanathan, C. Sairam Sundaram, and S. Meenakshi, "Removal of fluoride from aqueous solution using protonated chitosan beads," *Journal of Hazardous Materials*, vol. 161, no. 1, pp. 423–430, 2009.

[41] H. Valdés, M. Sánchez-Polo, and C. A. Zaror, "Impacto del tratamiento con ozono sobre las propiedades superficiales del carbón activado," *Ingeniare. Revista Chilena de Ingeniería*, vol. 19, no. 2, pp. 174–185, 2011.

[42] L. Giraldo and J. C. Moreno, "Relación entre la entalpía de inmersión de un carbón activado en soluciones acuosas de Pb^{2+} y los parámetros de adsorción," *Revista Colombiana de Química*, vol. 35, no. 1, pp. 41–49, 2006.

[43] N. Viswanathan, C. S. Sundaram, and S. Meenakshi, "Sorption behaviour of fluoride on carboxylated cross-linked chitosan beads," *Colloids and Surfaces B: Biointerfaces*, vol. 68, no. 1, pp. 48–54, 2009.

[44] N. Viswanathan, C. Sairam Sundaram, and S. Meenakshi, "Development of multifunctional chitosan beads for fluoride removal," *Journal of Hazardous Materials*, vol. 167, no. 1–3, pp. 325–331, 2009.

[45] Y. S. Ho, J. F. Porter, and G. McKay, "Equilibrium isotherm studies for the sorption of divalent metal ions onto peat: copper, nickel and lead single component systems," *Water, Air, and Soil Pollution*, vol. 141, no. 1–4, pp. 1–33, 2002.

[46] C. Gerente, V. K. C. Lee, P. Le Cloirec, and G. McKay, "Application of chitosan for the removal of metals from wastewaters by adsorption—mechanisms and models review," *Critical Reviews in Environmental Science and Technology*, vol. 37, no. 1, pp. 41–127, 2007.

[47] R. Bhattacharyya and S. K. Ray, "Removal of congo red and methyl violet from water using nano clay filled composite hydrogels of poly acrylic acid and polyethylene glycol," *Chemical Engineering Journal*, vol. 260, pp. 269–283, 2014.

[48] B. Kayranli, "Adsorption of textile dyes onto iron based waterworks sludge from aqueous solution; isotherm, kinetic and thermodynamic study," *Chemical Engineering Journal*, vol. 173, no. 3, pp. 782–791, 2011.

[49] Y. Liu and Y.-J. Liu, "Review: Biosorption isotherms, kinetics and thermodynamics," *Separation and Purification Technology*, vol. 61, no. 3, pp. 229–242, 2008.

[50] V. Vimonses, S. Lei, B. Jin, C. W. K. Chow, and C. Saint, "Kinetic study and equilibrium isotherm analysis of Congo Red adsorption by clay materials," *Chemical Engineering Journal*, vol. 148, no. 2-3, pp. 354–364, 2009.

[51] W. S. W. Ngah and S. Fatinathan, "Adsorption characterization of Pb(II) and Cu(II) ions onto chitosan-tripolyphosphate beads: kinetic, equilibrium and thermodynamic studies," *Journal of Environmental Management*, vol. 91, no. 4, pp. 958–969, 2010.

[52] M. Erşan, E. Baĝda, and E. Baĝda, "Investigation of kinetic and thermodynamic characteristics of removal of tetracycline with sponge like, tannin based cryogels," *Colloids and Surfaces B: Biointerfaces*, vol. 104, pp. 75–82, 2013.

[53] K. U. Ahamad and M. Jawed, "Kinetics, equilibrium and breakthrough studies for Fe(II) removal by wooden charcoal: a low-cost adsorbent," *Desalination*, vol. 251, no. 1-3, pp. 137–145, 2010.

[54] P. Liang, Y. Zhang, D. Wang, Y. Xu, and L. Luo, "Preparation of mixed rare earths modified chitosan for fluoride adsorption," *Journal of Rare Earths*, vol. 31, no. 8, pp. 817–822, 2013.

[55] J. Ma, Y. Shen, C. Shen, Y. Wen, and W. Liu, "Al-doping chitosan-Fe(III) hydrogel for the removal of fluoride from aqueous solutions," *Chemical Engineering Journal*, vol. 248, pp. 98–106, 2014.

[56] A. S. Elsherbiny, "Adsorption kinetics and mechanism of acid dye onto montmorillonite from aqueous solutions: stopped-flow measurements," *Applied Clay Science*, vol. 83-84, pp. 56–62, 2013.

[57] J. Thilagan, S. Gopalakrishnan, and T. Kannadasan, "Thermodynamic study on adsorption of Copper (II) ions in aqueous solution by Chitosan blended with Cellulose & cross linked by Formaldehyde, Chitosan immobilised on Red Soil, Chitosan reinforced by Banana stem fibre," *International Journal of Scientific Research Engineering & Technology*, vol. 2, no. 1, 2013.

[58] X. Li, Y. Li, S. Zhang, and Z. Ye, "Preparation and characterization of new foam adsorbents of poly(vinyl alcohol)/chitosan composites and their removal for dye and heavy metal from aqueous solution," *Chemical Engineering Journal*, vol. 183, pp. 88–97, 2012.

[59] R. Cortés-Martínez, M. T. Olguín, and M. Solache-Ríos, "Cesium sorption by clinoptilolite-rich tuffs in batch and fixed-bed systems," *Desalination*, vol. 258, no. 1–3, pp. 164–170, 2010.

[60] G. O. El Sayed and H. A. Dessouki, "Biosorption of Ni (II) And Cd (II) ions from aqueous solutions onto rice straw," *Chemical Sciences Journal*, vol. CSJ-9, pp. 1–11, 2010.

[61] M. Alkan, Ö. Demirbaş, and M. Doğan, "Adsorption kinetics and thermodynamics of an anionic dye onto sepiolite," *Microporous and Mesoporous Materials*, vol. 101, no. 3, pp. 388–396, 2007.

[62] N. Viswanathan and S. Meenakshi, "Synthesis of Zr(IV) entrapped chitosan polymeric matrix for selective fluoride sorption," *Colloids and Surfaces B: Biointerfaces*, vol. 72, no. 1, pp. 88–93, 2009.

[63] M. D. Burghardt, *Ingeniería Termodinámica*, 2nd edition, 1984.

[64] J. M. Smith, H. C. Van Ness, and M. M. Abbott, *Introducción a la Termodinámica en Ingeniería Química*, Mcgraw-Hill, Ciudad de México, México, 5th edition, 1997.

[65] M. Al-Ghouti, M. A. M. Khraisheh, M. N. M. Ahmad, and S. Allen, "Thermodynamic behaviour and the effect of temperature on the removal of dyes from aqueous solution using modified diatomite: A Kinetic Study," *Journal of Colloid and Interface Science*, vol. 287, no. 1, pp. 6–13, 2005.

[66] G. Crini and P.-M. Badot, "Application of chitosan, a natural aminopolysaccharide, for dye removal from aqueous solutions by adsorption processes using batch studies: a review of recent literature," *Progress in Polymer Science*, vol. 33, no. 4, pp. 399–447, 2008.

[67] N. Pérez, J. González, and L. A. Delgado, "Estudio termodinámico del proceso de adsorción de iones de Ni y V por parte de ligninas precipitadas del licor negro Kraft," *Revista Latinoamericana de Metalurgia y Materiales*, vol. 31, no. 2, pp. 168–181, 2011.